Published in final edited form as:
Dev Cell. 2012 January 17; 22(1): 104–115. doi:10.1016/j.devcel.2011.10.013.

A Mechanoresponsive Cadherin-Keratin Complex Directs Polarized Protrusive Behavior and Collective Cell Migration

Gregory F. Weber[1], **Maureen A. Bjerke**[1], and **Douglas W. DeSimone**[1]
[1]Department of Cell Biology, School of Medicine, University of Virginia Health System, Charlottesville, Virginia 22908

Summary

Collective cell migration requires maintenance of adhesive contacts between adjacent cells, coordination of polarized cell protrusions, and generation of propulsive traction forces. We demonstrate that mechanical force applied locally to C-cadherins on single *Xenopus* mesendoderm cells is sufficient to induce polarized cell protrusion and persistent migration typical of individual cells within a collectively migrating tissue. Local tension on cadherin adhesions induces reorganization of the keratin intermediate filament network toward these stressed sites. Plakoglobin, a member of the catenin family, is localized to cadherin adhesions under tension and is required for both mechanoresponsive cell behavior and assembly of the keratin cytoskeleton at the rear of these cells. Local tugging forces on cadherins occur *in vivo* through interactions with neighboring cells, and these forces result in coordinate changes in cell protrusive behavior. Thus, cadherin-dependent force-inducible regulation of cell polarity in single mesendoderm cells represents an emergent property of the intact tissue.

Embryos undergo dramatic cell and tissue rearrangements that are required for sculpting the embryonic body plan. These underlying movements result in the generation of forces that are sensed both locally and globally by other cells and tissues in the embryo. Mechanotransduction is the cellular process responsible for converting these forces to chemical and electrical signals. Thus, physical force may serve to instruct and guide key aspects of development including gene expression, differentiation, cell polarity and morphogenesis (Schwartz and DeSimone, 2008; Mammato and Ingber, 2010). Despite the likely importance of force and mechanotransduction to embryogenesis and development, relatively few specific examples of embryonic processes directed by mechanical inputs have been reported thus far.

Many diverse tissue types, including epithelial cell sheets (Farooqui and Fenteany, 2005), cords of metastatic cells (Wolf et al., 2007), neural crest cells (Theveneau et al., 2010), lateral line primordia (Haas and Gilmour, 2006) and mesendoderm of the *Xenopus* gastrula (Davidson et al., 2002), undergo collective cell migration and the morphological features of these events are remarkably conserved. Leading edge protrusions of each cell within the tissue are in contact with the extracellular matrix while the rear or “retracting” edge of each cell rests upon the leading edge of the cell behind it in a shingle-like arrangement (Figure 1A). Frog mesendoderm tissue migrates on fibronectin (FN) matrix and like other

Address correspondence to Douglas W. DeSimone. Tel: (434)-924-2172. Fax: (434)-982-3912. desimone@virginia.edu.

collectively migrating populations of cells, the fidelity of mesendoderm movement requires cell-cell contact. When cells from this tissue are dissociated from one another and plated on FN they become multi-polar, protrude randomly and migrate with erratic speed and direction (Nakatsuji and Johnson, 1982; Winklbauer et al., 1992). Chemotactic and haptotactic cues that may influence directional migration of intact mesendoderm are not sufficient to guide migration of single mesendoderm cells (Winklbauer, 1990; Winklbauer et al., 1992), further highlighting the importance of cell-cell contact in this process.

Collectively migrating tissues generate traction forces and advance against tensile forces distributed along cell-cell adhesive contacts. *Xenopus* mesendodermal explants migrate collectively on FN substrates and perturbation of integrin-FN adhesion causes a rapid unidirectional retraction of the cell sheet (Davidson et al., 2002). The retraction of the mesendodermal sheet occurs opposite the direction of mesendoderm migration and perpendicular to both the leading edge of the mesendoderm and the blastopore lip. The directional nature of tissue retraction under these conditions indicates that the intercellular tension in the mesendoderm tissue is asymmetric, being greatest in the axis of migration and weaker in the mediolateral axis. Recent studies of migrating MDCK cell sheets reveal a similar asymmetry of tension within the sheet and find greater forces applied to cell-cell contacts in the rows of cells behind those at the leading edge (Trepat et al., 2009). The implications of this force asymmetry for tissue morphogenesis are not known.

Classical cadherins enable cell-cell cohesion and allow development of migratory polarity in epithelial cell sheets *in vitro* (Desai et al., 2009; Dupin et al., 2009), however, the potential involvement of mechanical force on cadherin adhesions in these contexts has not been addressed. Cadherins have been reported to sense and respond to mechanical force by eliciting a strain-stiffening response (le Duc et al., 2010; Liu et al., 2010). Integrins are well known to be involved in mechanotransduction (Moore et al., 2010; Schwartz and DeSimone, 2008), but only recently have cadherins also been implicated as important mediators of mechanical stimuli (le Duc et al., 2010; Yonemura et al., 2010). We hypothesize that asymmetries in tension on cadherins are an intrinsic consequence of tissues undergoing bulk movement or deformation and that these mechanical signals induce the establishment of cell protrusive polarity and directed migration.

Association of cadherins with the cytoskeleton provides both mechanical strength at points of adhesion and scaffolds for proteins involved in cell signaling. Binding of catenin family members, such as β-catenin or plakoglobin (PG; also known as γ-catenin), to the cytoplasmic tail of cadherins enables recruitment of cytoskeletal filaments to sites of cell-cell contact. Both β-catenin and PG can facilitate the association of classical cadherins with the actin cytoskeleton (Hirano et al., 1987). PG, unlike β-catenin, can also enable classical cadherin associations with intermediate filaments (IFs) (Kowalczyk et al., 1998; Leonard et al., 2008). While the linkage between cadherins and actin filaments has been studied extensively, the functional significance of IF-associated classical cadherin adhesions is not well understood. In this study we demonstrate that local forces applied to C-cadherins result in the PG-dependent recruitment of keratin IFs (KIFs), and that this mechanically responsive linkage is required for the directed protrusive behavior of individual cells within the collectively migrating mesendoderm.

Results

Pulling on C-cadherin Induces Directional Protrusions

We used a magnetic tweezer to apply local pulling forces to cadherin adhesions and analyzed the impact of this manipulation on cell polarity and migratory behavior (Figure 1B). A key advantage of this approach over prior studies of cadherin involvement in

migratory cell polarity (Borghi et al., 2010; Desai et al., 2009; Dupin et al., 2009) is the ability to distinguish between effects due only to cadherin engagement (bead attached/without pull) and those due to force on cadherin adhesions (bead pulled). C-cadherin (Cdh3) is the primary cadherin expressed in *Xenopus* gastrulae and is required for maintaining cell cohesion and tissue integrity (Heasman et al., 1994). Single paramagnetic beads coated with the extracellular domain of C-cadherin (C-cadFc) were placed alongside individual dissociated mesenoderm cells plated on FN. Cells were allowed 20 minutes to bind the beads and the attached beads were subsequently pulled with the magnetic tweezer (Figure 1B,S1).

Application of mechanical force to C-cadherin adhesions restored the normal *in vivo* morphology of these migratory cells. When mesendoderm is dissociated to single cells they lose the characteristic monopolar protrusive behavior exhibited *in vivo* (Figure 1A) and become multipolar protrusive in random orientation (Figure 1C, Movie S1). C-cadFc bead attachment alone had no effect on protrusive orientation [p(rand)=0.749] (Figure 1D,F, Movie S2). When force was applied to the bead, protrusions became markedly biased opposite the direction of pull [p(rand)=0.002] (Figure 1E,F; Movie S2). The cells then migrated persistently away from the direction of the applied force. Additionally, there was a reduction in the total number of protrusions from each cell upon bead pull (Figure 1G), reflecting the monopolar protrusive behavior exhibited by mesendoderm cells *in vivo*.

Pulling with ~1.5 nN of force per 22.9 μm bead was sufficient to induce cell polarization. This force is about one order of magnitude less than the forces calculated between MDCK cell pairs on FN substrate (Maruthamuthu et al., 2011). However, if we assume that a mesendoderm cell binds ¼ to ½ of the surface of a C-cadFc bead then 2-4 Pa of stress is being applied to mesendoderm cells in our bead pull assay, an amount comparable to the tugging stresses of 5 Pa reported for MDCK epithelial sheets (Trepat et al., 2009).

We also noted that individual mesendoderm cells were able to respond to repeated cycles of force application suggesting a significant degree of plasticity with regard to this mechanoresponsive behavior (Movie S3). Force was applied to cadherin adhesions and then halted once monopolar protrusive behavior was induced. Cells rapidly reverted to multipolar protrusive behavior when force application ceased, typically within one or two minutes. Subsequent application of force re-induced monopolar protrusions away from the direction of the applied force. Similarly, single mesendoderm cells became monopolar protrusive when they formed adhesions with neighboring cells and reverted back to a multipolar state as these adhesions were broken (Movie S4). Monopolar protrusive behavior was evident in >50% of cells within 5-10 minutes, but took as long as 20 minutes to develop in others. Once established, this protrusive behavior persisted until force on cadherin adhesion ceased or the cohesive bond was broken.

Force Induction of Cell Protrusions is Specific to Cadherin Adhesions

Because force was required to alter the polarity of protrusions, tension on the cell cortex is clearly a critical stimulus. However, it was unclear whether this response required signaling through cadherins or was a general consequence of pulling on the cell surface. Pulling on poly-L-lysine (PLL) coated beads attached to mesendoderm cells was not sufficient to alter cell protrusive orientation [p(same)=0.933] (Figure S2A). We also evaluated whether engagement and application of force to other adhesion molecules could elicit a response. Force application to syndecans or integrins, via beads coated with the HepII (Hep2FN) or RGD-containing central cell binding (9.11FN) domains of FN, respectively, was unable to induce the polarized protrusive behavior observed with C-cadFc beads (Figure S2B-D). These results indicate that the mechanical stimulation of monopolar protrusive activity and

directional cell migration is specifically associated with signaling through C-cadherin adhesions.

Keratin Localization to Stressed Cadherin Adhesions Correlates with Cell Polarity

Cadherins associate with cytoskeletal networks, including actin (Hirano et al., 1987) and IFs (Kowalczyk et al., 1998; Leonard et al., 2008), to provide both mechanical strength at points of adhesion and scaffolds for proteins involved in cell signaling. IFs in particular exhibit high tensile strength (Kreplak et al., 2008) and KIFs are well-known to impart mechanical resilience to cells (Coulombe et al., 1991). We found that the organization of KIFs in mesendoderm was tightly correlated with cell polarity and directed cell movements. KIFs in isolated cells were distributed randomly and lacked obvious orientation (Figure 2A). However, when mesendoderm cells *in vitro* were in contact with their neighbors KIFs were noted at discrete points along cell-cell interfaces (Figure 2B). The correlation between cell protrusive polarity and reorganization of KIFs toward the points of cell-cell contact was particularly striking in live cells expressing GFP-labeled keratin (Movie S4). KIFs aggregated near cell-cell contacts as cells formed protrusions in directions opposite these cell-cell boundaries. Cells in mesendoderm explants also had KIFs concentrated at the rear of each cell (Figure 2C). Filaments were organized in a basket-like arrangement along the posterior-basolateral surface and were associated with the cell membrane at points of cell-cell contact. A similar organization of KIFs was evident in mesendoderm cells in sagittally bisected gastrula-stage embryos (Figure 2D). An additional feature of keratin organization in whole tissues was the arrangement of KIFs into bundles perpendicular to the forward axis of migration but only in the row of cells that comprised the advancing front of the mesendoderm tissue (Figure 2C). This KIF cabling parallel to the leading edge closely resembles what has been observed in some epithelial cell sheets *in vitro* (Long et al., 2006).

Binding of C-cadFc beads to mesendoderm cells had no effect on the localization of KIFs (Figure 2E) but when force was applied to these beads, KIFs were reorganized to the posterior of the cell proximal to the site of bead pull (Figure 2E’). A similar reorganization of KIFs was observed when two dissociated cells on FN formed a cell-cell adhesion *in vitro*. The cells polarized and moved in opposite directions but remained adherent while tugging on one another (Figure 2F). As observed with C-cadFc bead pull, KIFs were recruited to the rear of these cells where force was being generated at the point of cell-cell contact as a consequence of traction forces on the FN substrate (Figure 2B,G; Movie S4). In contrast, cell pairs plated on PLL substrate are unable to generate substrate traction; they did not exhibit directed protrusive activity and failed to reorganize KIFs toward the cell-cell boundary (Figure 2H). We conclude that mechanical forces applied to C-cadherin adhesions induce both directional protrusive behaviors and KIF reorganization toward the posterior of the newly polarized cell.

Keratin and PG are Required for Force-Induced Polarized Cell Protrusive Behavior

To address whether KIFs are part of the molecular machinery that specifies polarity in these cells in response to a pulling force on C-cadherin, antisense morpholinos were used to knockdown expression of XCK1(8), also known as Krt8 (Figure S3A). KIFs are obligate heteropolymers comprised of type I acidic and type II basic cytokeratin proteins. Early *Xenopus* gastrulae express multiple type I cytokeratins (Franz et al., 1983), but XCK1(8) is the only type II cytokeratin expressed at these stages of development (Franz and Franke, 1986). Dissociated mesendoderm cells from XCK1(8) morphant embryos were unresponsive to C-cadFc bead pull (Figure 3A, Movie S5). Moreover, directed protrusive activity was perturbed throughout intact mesendoderm explants derived from these embryos (Figure 3B, Movie S6). The lack of response to bead pull was confirmed using a second morpholino (XCK MO-2) targeting a different sequence in the XCK1(8) mRNA (Figure S3A-C). Intact

XCK1(8) morphant embryos exogastrulated (Figure S3D,E), a phenotype that closely parallels that reported in earlier studies targeting either keratin protein expression (Torpey et al., 1992) or filament assembly and organization (Klymkowsky et al., 1992) in *Xenopus*. Exogastrulation could be partially rescued by co-injection of antisense morpholino (XCK MO-1) and a GFP-tagged XCK1(8) transcript lacking the target sequence (Figure S3D,E). As in other studies (Torpey et al., 1992), we were unable to achieve complete knockdown of endogenous keratin due to maternal expression and slow turnover of keratin protein. However, the severity of morphant phenotypes arising from partial keratin knockdown suggests that maintenance of normal XCK1(8) protein levels is critical for mechanoresponsive cellular behavior and normal gastrulation movements. Together these data demonstrate that KIFs are necessary for the induction of cell polarity and directed cell movements following application of force to C-cadherin adhesions.

Cadherins are linked to cytoskeletal networks through members of the catenin family of proteins. PG is known to associate with both desmosomal and classical cadherins, and is a component of the less-well understood classical cadherin complexes that associate with IFs (Kowalczyk et al., 1998; Leonard et al., 2008). As observed in the XCK1(8) knockdown experiments, inhibition of PG expression with antisense morpholinos (Figure S4) resulted in failure of single mesendodermal cells on FN to respond to C-cadFc bead pull by repolarizing (Figure 3C, Movie S7). PG knockdown was also associated with an increase in the number of protrusions relative to control cells ($p<0.001$) and this increase was not affected by bead pull (Figure 3D). Todorovic et al (2010) noted a similar increase in protrusive activity in PG-null keratinocytes, which they attributed to increased Rac activity.

Lamellipodial protrusions in the direction of tissue migration (180°) are evident in both leading edge cells and following cells in normal intact mesendoderm. In control morpholino explants, the angular variance of protrusions between leader cells and following cells was not statistically significant (Figure 3E). In other words, both types of cells show spatially well-oriented protrusion behaviors. Intact mesendoderm explants from PG knockdown embryos retained polarized protrusions in leader cells in the general direction of migration (Figure 3F; Movie S8). However, protrusions of follower cells in PG morphant explants were significantly more broadly distributed than those of leader cells [$p(same)=0.001$]. These data indicate that PG has a role in regulating mesendodermal cell polarity but suggest that additional factors are also involved in maintaining the polarized behaviors of cells in intact mesendoderm.

PG is Recruited to C-cadherin Adhesions Under Tension

Because PG knockdown prevented mesendoderm cells from responding to C-cadFc bead pull, we next examined whether force on C-cadherin adhesions could induce the local recruitment of PG in normal cells. Discrete punctae of PG-GFP were observed at the plasma membrane in proximity with the C-cadFc bead when force was applied (Figure 4A,A'). As a complimentary approach and to confirm results obtained through bead pull, we utilized the cell tugging assays described earlier (Figure 2F-H) to visualize accumulation of C-cadherin and PG at cell-cell adhesion interfaces under conditions that permitted (i.e. FN) or precluded (i.e. PLL) the generation of cell traction forces on the substrate. PG was observed along the cell-cell boundaries of cell pairs that were plated on FN substrates and allowed to polarize, generate traction force and protrude in opposing directions (Figure 4B). In contrast, PG was not detected at cell-cell adhesions in cell pairs plated on PLL (Figure 4B'). C-cadherin was present at points of cell-cell contact regardless of whether cell pairs formed on FN or PLL (Figure 4C,C'). Thus we conclude that the recruitment of PG to C-cadherin adhesions specifically requires the application of force.

After observing the force-dependent recruitment of PG to cell-cell contacts *in vitro*, we examined the localization of PG to C-cadherin/KIF complexes in intact mesendoderm tissues. In mesendoderm tissue explants, PG formed punctate plaques at cell boundaries and KIFs co-localized at these discrete locations (Figure 4D). These points of contact were found at the lateral and posterior contacts between mesendoderm cells. Co-immunoprecipitation analysis confirmed that PG was indeed associated with C-cadherin in *Xenopus* gastrulae (e.g., Figure 4E). PG associated with C-cadherin and localized with KIFs in a pattern consistent with a role for PG in mediating a mechanoresponsive linkage between C-cadherin and the KIF network.

PG Mediates C-cadherin Association with Keratin

We next investigated whether PG plays a role in linking KIFs to mechanically stimulated cadherins in the mesendoderm. Cells from control or PG morphant embryos were subjected to C-cadFc bead pull and KIFs were imaged. The KIF cytoskeleton in both control and PG morphant cells was distributed broadly throughout the cytoplasm prior to the application of force to attached C-cadFc beads (Figure 5A,B). In contrast to controls, KIFs in PG knockdown cells did not reorganize toward the direction of bead pull when force was applied (Figure 5A',B').

PG was also required for normal KIF organization in intact mesendoderm tissues. We expressed GFP-tagged XCK1(8) and used timelapse imaging of live mesendoderm explants to resolve KIF organization following knockdown of PG expression. In control morpholino explants, KIFs were located basally and associated with discrete points of cell-cell contact in the posterior half of each cell (Figure 5C,S5A; Movie S8). A band of KIFs also spanned the anterior leading edge of cells perpendicular to the direction of tissue movement as noted earlier (Figure 2C). In PG morphant explants, KIFs were more broadly distributed and lacked clear points of association with cell-cell contacts, however, the arrangement of KIFs along the anterior margins of the leading edge cells persisted (Figure 5D,S5B; Movie S8). KIF organization was similarly disrupted in the mesendoderm of PG morphant embryos (Figure 5E,F). This suggests that PG-dependent and -independent mechanisms are involved in organizing these two distinct populations of filaments. Thus, the persistence of KIF cabling at the front of leading-edge cells in the absence of PG may have contributed to the general maintenance of directed cell protrusions observed in tissue explants (Figure 3F), whereas keratin knockdown disrupted cell protrusion orientation in leader and follower cells alike (Figure 3B).

Co-immunoprecipitation analyses were performed to explore further the putative PG-dependent linkage of C-cadherin to KIFs in these embryos. GFP-tagged XCK1(8), which is incorporated into endogenous KIFs (Clarke and Allan, 2003), associated with C-cadherin obtained from control lysates (Figure 5H,I). Knockdown of PG expression (Figure 5G) significantly reduced XCK1(8)-GFP association with C-cadherin ($p<0.05$) (Figure 5H,I). Altogether these data implicate PG as a key factor that mediates C-cadherin force-induced cell polarity and KIF reorganization.

PG and Keratin are Required for Normal Mesendoderm Polarity and Organization *In Vivo*

Pulling on C-cadherin was sufficient to induce directional polarity of mesendoderm cells *in vitro*, and keratin and PG were required for the force-dependent polarization of migratory mesendoderm cells in both isolated cells and in explanted tissue. In order to investigate whether this mechanism is likely involved in normal mesendoderm migration *in vivo*, mesendoderm morphology was examined in whole embryos following knockdown of either XCK1(8) or PG. Morphant embryos were fixed at mid-gastrulation and examined by scanning electron microscopy. In the embryo, mesendoderm cells crawl on a FN matrix

assembled by the ectodermal cells of the blastocoel roof. Removal of the blastocoel roof post-fixation revealed the basal aspect of the mesendoderm, which is the surface normally in contact with the FN matrix but obscured by the blastocoel roof (Figure 6). The mesendoderm of control morphant embryos was organized as reported previously by others (Keller and Schoenwolf, 1977; Nakatsuji, 1975) with polarized protrusions in the direction of tissue migration and "follower" cells that underlapped the cells in front of them, creating a "shingled" organization characteristic of this tissue (Figure 6A). An oblique view of this tissue showed that cells appeared mostly elongate and rounded but extended flattened protrusions in the forward direction (Figure 6D). In contrast, mesendoderm cells from both PG and XCK1(8) morpholino-injected embryos exhibited a greater number of discrete protrusions per cell and were less well shingled with fewer underlapping cells than controls. These protrusions were frequently oriented away from the direction of tissue migration (Figure 6B,C). The basal surfaces of cells from these embryos were also more flattened than controls (Figure 6E,F), perhaps due to increased randomized protrusive activity and cell spreading along the blastocoel roof. These results are consistent with a role for PG and keratin in force-induced directional protrusive activity and migration of mesendoderm *in vivo*.

Discussion

Our identification of local force application on cadherins as an inductive signal for cell polarity offers some mechanistic insight into nearly 60 years of observations on the role of cell-cell contacts in directing cell migration (Abercrombie and Heaysman, 1953; Desai et al., 2009; Dupin et al., 2009; Kolega, 1981; Arboleda-Estudillo et al., 2010). By applying tension to cadherin-based adhesions using a magnetic tweezer, a mechanical asymmetry was initiated in the cell that induced polarized protrusions and necessary tractions to resolve the imbalance of forces (Figure 7A). A similar phenomenon was also observed in cell pairs (Figure 7B) where forces at the cell-cell boundary are counterbalanced by traction forces biased away from the cell-cell interface (Liu et al., 2010; Maruthamuthu et al., 2011).

How then do forces on cell-cell contacts promote polarized protrusions in the *same* direction as in the mesendoderm or epithelial sheets where a morphological "shingling" of underlapping cells occurs? For each cell in the migrating sheet, force is greater on cell-cell contacts at the rear than on cell-cell contacts at the front (Trepat et al., 2009). In the leading edge cells, this asymmetry is obvious because cadherin adhesions themselves are isolated to the rear and lateral sides of each cell. In subsequent rows cadherin adhesions exist around the entire perimeter of each cell (Angres et al., 1991), but force on cadherin adhesions is greatest in the trailing ends rather than the leading edges of each cell in the collectively migrating array (Trepat et al., 2009). Thus, force on cell-cell adhesions is asymmetric even though the overall *presence* of cell-cell adhesions is symmetric. This is consistent with our conclusion that cadherin engagement alone is not sufficient to induce mesendoderm cell polarity and that force on the cadherin adhesion is the key stimulus. We suggest that force imbalance between cadherin adhesions at the front and rear of each cell is an intrinsic property of the migratory cell sheet that stimulates directed cell protrusions.

If mesendoderm is migrating against an intercellular tension that builds within the tissue, then what balances the force in the opposing direction? As Trepat et al (2009) report, in simple epithelial culture models, opposite sides of a cell aggregate exert tractive stresses on the substrate in opposing directions (i.e., cells at margins of epithelial "islands" migrate radially away from the center of the cell aggregate) to balance intercellular stresses (Trepat et al., 2009) (Figure 7C). In the case of the mesendoderm, however, this tissue is an integral part of a larger embryo comprised of multiple tissue types. Behind the migratory mesendoderm (i.e., in both the embryo and the tissue explants used in these studies) are the

mesodermal cells, which in the dorsal region of the gastrula, intercalate mediolaterally and are oriented perpendicular to the movement of the mesendoderm (Figure 1A). We speculate that the trailing mesoderm acts to “anchor” the mesendoderm by providing resistance to the cell-cell forces and migratory traction forces being generated within the latter (Figure 7D). Interestingly, mesendoderm explants lacking these trailing mesoderm tissues fail to migrate directionally on FN and instead spread radially in all directions (Winklbauer, 1990) as we would predict from our model.

Because cooperative migratory behaviors require both cohesion and force application at the cell-cell interface, we propose the term “cohesotaxis” to describe this form of motility. Force imbalance on cadherin adhesions is an implicit component of this guidance mechanism. Examples of cohesotaxis would include cell groups with seemingly disparate phenotypes, such as cells that migrate away from one another (e.g., Figure 2F) or that migrate cooperatively in a unified direction in response to cohesive interactions [e.g., intact mesendoderm (Davidson et al., 2002), epithelial sheets (Farooqui and Fenteany, 2005), and *Drosophila* border cells (Prasad and Montell, 2007)].

Directed movement of the mesendoderm *in vivo* has been reported to require a gradient of of ECM-bound platelet-derived growth factor (PDGF) deposited along the blastocoel roof on which the tissue migrates (Nagel et al., 2004). While such a chemotactic mechanism may contribute to directed motility, we and others have observed that mesendoderm explants are still able to migrate directionally on isotropic FN substrates lacking PDGF (Davidson et al., 2002; Winklbauer, 1990). Moreover, isolated single mesendoderm cells do not orient or migrate directionally on blastocoel roof explants or substrates conditioned with blastocoel roof matrix (Winklbauer, 1990; Winklbauer et al., 1992), which contain PDGF and any other factors that may be involved in chemotaxis (or haptotaxis) *in vivo*. We conclude that a chemotactic mechanism is alone insufficient to account for directed mesendoderm migration in the absence of cell cohesion. One possibility is that a gradient of PDGF is contributing to this process by modulating cadherin adhesion as in other systems (McDonald et al., 2003; Theisen et al., 2007; Yang et al., 2008).

A key step in the cellular response to tensile force stimulation is the recruitment of PG to C-cadherin adhesions under stress. In the mesendoderm, PG is required for normal organization of the cellular KIF network and facilitates association of KIFs with C-cadherin. PG is an adaptor protein that contains multiple armadillo repeats, which are involved in direct binding to classical and desmosomal cadherins, as well as the keratin-binding proteins desmoplakin and plakophilin (Bonne et al., 2003; Choi et al., 2009; Kowalczyk et al., 1997). Thus, PG may function as a key physical link between the KIF cytoskeleton and classical cadherins such as C-cadherin. While current evidence supports this hypothesis an alternative possibility is that PG functions indirectly, perhaps by signaling changes in IF assembly and/or organization.

We have shown that polarized cellular protrusions are formed in response to mechanical stimulation but the molecular components of the initiating mechanosensor(s) involved remain unclear. C-cadherin is one obvious candidate given that the observed morphological response requires specific application of force through cadherin adhesions. Signaling events proximal to the site of force application could involve direct conformational changes in C-cadherin or associated proteins that link C-cadherin to the cytoskeletal and/or signaling machinery within the cell. Alternatively, tugging on cadherin adhesions might increase the local accumulation of cadherins at the site of applied force. Indeed in some cells, the size of cadherin-based adhesions correlates with the magnitude of forces exerted by these adhesions (Ladoux et al., 2010; Liu et al., 2010). An accumulation of cadherin complexes at sites of local mechanical stress could facilitate the recruitment PG and KIFs to these sites as well.

This mechanism may not require immediate (e.g., milliseconds to seconds) activation of a "mechanosensor" complex per se, but rather a more gradual (e.g., seconds to minutes) cellular response to an initiating mechanical stimulus.

It is remarkable that the organization of the KIF network is sensitive to mechanical stimuli and has a role in specifying migration polarity. Long et al (2006) previously observed that keratin-8 knockdown with siRNA inhibited directional migration of MCF-7, HeLa and Panc-1 epithelial cell sheets. This effect on migration was accompanied by irregular cell spreading and perturbation of cell-cell contacts that allowed cells to migrate individually in a randomized manner (Long et al., 2006). Likewise, keratinocytes null for K6 are more fragile than control cells and exhibit increased motility (Wong and Coulombe, 2003). While XCK1(8)-morphant mesendoderm remained a cohesive tissue, cell protrusive behavior and directional migration were disrupted, suggesting that KIFs have a more specialized function than simple maintenance of tissue integrity.

PG and KIFs associated with C-cadherin adhesions at discrete foci (e.g., Figures 2B and 4D) and in response to increased mechanical tension (Figures 4 and 5), suggesting the presence and dynamic assembly-disassembly of nascent desmosome-like adhesions in a rapidly migrating tissue. Thus, C-cadherin in these cells is involved in both adherens and desmosome-like adhesive specializations, where both rapid molecular dynamics typical of classical cadherins and enhanced load-bearing typical of IF linkages may exist. The functional interplay of mechanisms regulating the adhesive and mechanical properties of cells in the mesendoderm is likely shared by other tissues undergoing collective forms of cell migration. In the case of wound healing, such changes may be achieved through differential expression of keratin pairs (Wong and Coulombe, 2003) with unique viscoelastic properties (Yamada et al., 2002; Hofmann and Franke, 1997). Stiffness of KIF networks can also be modulated by filament bundling (Yamada et al., 2002). IF function and organization are deeply integrated with the activities of many cell signaling pathways. Several extracellular ligands, including the bioactive lipid sphingosylphosphorylcholine (SPC), have been shown to induce migration of single cells, accompanied by collapse of the KIF network into a perinuclear-concentrated ring (Beil et al., 2003). Moreover, SPC-treated cells have a marked decrease in the elastic modulus, supporting the notion that IFs serve as tensile elements in living cells (Beil et al., 2003).

IFs are also reported to be regulated by RhoGTPases. Local activation of Rac1 promotes the disassembly of vimentin IFs, which induces lamellipodial protrusion in the "front" of the cell. Meanwhile, assembled IFs are maintained at the "rear" (Helfand et al., 2011). Other recent studies show that Rac activity is negatively regulated by both PG (Todorovic et al., 2010) and cadherin adhesion (Kitt and Nelson, 2011). We suggest that anterior-posterior orientation could be established by the stabilization of KIFs through the local inhibition of Rac by PG at sites of stressed cell-cell contacts while allowing KIF depolymerization and lamellipodial extension in the presumptive front of the cell. The contribution of mechanical stimulation of cadherins to regulation of Rac activity and the related effects on IFs are an important line of future investigation. Continued efforts in these areas will be needed to elucidate the many structural and cell-signaling relationships involved in cohesotaxis.

Experimental Procedures (see Supplemental Experimental Procedures for more detail)

Xenopus egg and embryo preparation

Embryos were obtained and cultured using standard methods and staged according to Nieuwkoop and Faber (1994). Embryos were dejellied and cultured at 16°C in 0.1X modified Barth's saline.

Mesendoderm cell preparation

Glass coverslips were coated with bovine plasma FN (Calbiochem) or poly-L-lysine solution (Sigma). Dorsal mesendoderm tissue from stage 10 *Xenopus* embryos was dissociated in Ca^{2+}/Mg^{2+}-free 1X MBS. Dissociated cells were then transferred to 0.5X MBS containing Ca^{2+}/Mg^{2+} on FN-coated coverslips.

Dorsal marginal zone explant preparation

DMZ explants were prepared according to Davidson et al (2004). Briefly, stage 10 minus *Xenopus* gastrulae were placed in 0.5X MBS and lateral incisions were made to separate dorsal and ventral portions of the embryo. Vegetal cells were scraped away using an eyebrow knife, leaving behind the mesendodermal, mesodermal and bottle cells. The explants were placed on FN-coated coverslips and compressed from above with coverglasses supported and spaced with silicone grease. Explants were allowed to attach and begin migrating for 1 hour before image acquisition.

Magnetic bead pull assay

Superparamagnetic beads (Spherotech, Libertyville, IL) were covalently coated with Protein G (Calbiochem) followed by affinity binding of C-cadFc protein (Barry Gumbiner, University of Virginia) (Chappuis-Flament et al., 2001). Coated beads were transferred to dishes of mesendoderm cells and positioned by pipette. After cells attached to beads, a magnetic tweezer was used to pull beads with 1100-1500pN of force.

Protrusion quantification

Cell protrusions in isolated mesendoderm cells are readily identified by a lack of yolk platelets, which remain constrained to the cell body. Protrusion angles were measured using the cell centroid as the vertex of the angle, the right hand side of the frame (i.e. magnet position) as 0°, and the midline of the each protrusion as the final ray of the angle. Total protrusions from all cells were binned into 30° ranges and plotted as rose diagrams using OriginPro software. Y-axis for all rose diagrams represents percent of total protrusions. For quantification of cell protrusions in intact dorsal mesendoderm tissue, embryos were injected after fertilization with RNA encoding a membrane bound GFP (GAP43-GFP). Plasma membranes of cells comprising the tissue were then imaged by laser scanning confocal microscopy (see below for microscopy details). Acquired images were analyzed using ImageJ software to calculate the angles of protrusions. First, a ray was drawn perpendicular to the leading edge of the tissue and intersecting the estimated centroid of the cell being measured. A second ray was drawn extending from the cell centroid through the middle of each protrusion on that cell. Angular measurements were grouped into bins of 30°, where 180° is equivalent to the direction of tissue movement, and plotted in rose diagram format using OriginPro software. Y-axis for all rose diagrams represents percent of total protrusions. Protrusive orientation data was analyzed using two statistical measures: Rayleigh test for randomness [p(rand)] and Mardia-Watson-Wheeler test [p(same)] for non-parametric two-sample comparison (Batschelet, 1981). Statistical analysis of protrusive orientation data was performed using PAST software (Hammer et al., 2001).

RNA constructs, morpholinos and microinjection

RNA was transcribed *in vitro* from linearized plasmids. Transcripts were injected in 5nl doses containing ~500pg of RNA into one or two dorsal blastomeres at the two to four cell stage to target expression in mesendoderm. Morpholino oligodeoxynucleotides used to inhibit translation were obtained from GeneTools (Philomath, OR).

Immunofluorescence

Embryos and dissociated cells plated on FN were fixed in ice-cold 100% methanol or Dent's fixative (80% methanol, 20% DMSO). Samples were rehydrated by partial buffer changes with TBS. Embryos were blocked overnight with 10% goat serum, 1% BSA, 0.15% Triton X-100 diluted in PBS. Overnight primary antibody incubation was followed by goat anti-mouse and rabbit IgG conjugated to Alexa-488, -555 or -647 fluorophores (Molecular Probes). Bisected embryos were dehydrated in methanol and cleared in benzyl benzoate/benzyl alcohol for microscopy.

Western Blot

Whole *Xenopus* embryos were solubilized in lysis buffer (100 mM NaCl, 50 mM Tris-HCl pH 7.5, 1% Triton X-100, 2 mM PMSF (phenylmethylsulphonylfluoride), with protease inhibitor cocktail [Sigma]). Protein extracts were diluted in 2X Laemmli buffer (2% β-mercaptoethanol). One embryo-equivalent of protein per sample was resolved on a 7% SDS-PAGE gel and transferred to nitrocellulose for probing with antibodies.

Supplementary Material

Refer to Web version on PubMed Central for supplementary material.

Acknowledgments

We would like to thank the Advanced Microscopy Facility at University of Virginia for assistance in preparing samples and acquiring scanning electron micrographs. We also extend our gratitude to our colleagues: Bette Dzamba for her technical assistance with immunolocalization studies, Bill Guilford who provided advice regarding construction of the magnetic tweezer, Judy White and Rick Horwitz for reading and commenting on the manuscript, and to all of the colleagues who provided reagents used in these studies. This work was supported by USPHS grants F32-GM83542 to G.F.W., T32-GM08136 to M.A.B., and R01-HD26402/GM094793 to D.W.D.

References

Abercrombie M, Heaysman JE. Observations on the social behaviour of cells in tissue culture. I. Speed of movement of chick heart fibroblasts in relation to their mutual contacts. Exp Cell Res. 1953; 5:111–131. [PubMed: 13083622]

Angres B, Muller AH, Kellermann J, Hausen P. Differential expression of two cadherins in Xenopus laevis. Development. 1991; 111:829–844. [PubMed: 1879345]

Arboleda-Estudillo Y, Krieg M, Stühmer J, Licata NA, Muller DJ, Heisenberg CP. Movement directionality in collective migration of germ layer progenitors. Curr Biol. 2010; 20:161–169. [PubMed: 20079641]

Batschelet, E. Circular Statistics in Biology. London: Academic Press Inc; 1981.

Beil M, Micoulet A, von Wichert G, Paschke S, Walther P, Omary MB, Van Veldhoven PP, Gern U, Wolff-Hieber E, Eggermann J, et al. Sphingosylphosphorylcholine regulates keratin network architecture and visco-elastic properties of human cancer cells. Nat Cell Biol. 2003; 5:803–811. [PubMed: 12942086]

Bonne S, Gilbert B, Hatzfeld M, Chen X, Green KJ, van Roy F. Defining desmosomal plakophilin-3 interactions. J Cell Biol. 2003; 161:403–416. [PubMed: 12707304]

Borghi N, Lowndes M, Maruthamuthu V, Gardel ML, Nelson WJ. Regulation of cell motile behavior by crosstalk between cadherin- and integrin-mediated adhesions. Proc Natl Acad Sci U S A. 2010; 107:13324–13329. [PubMed: 20566866]

Chappuis-Flament S, Wong E, Hicks LD, Kay CM, Gumbiner BM. Multiple cadherin extracellular repeats mediate homophilic binding and adhesion. J Cell Biol. 2001; 154:231–243. [PubMed: 11449003]

Choi HJ, Gross JC, Pokutta S, Weis WI. Interactions of plakoglobin and β-catenin with desmosomal cadherins: basis of selective exclusion of α- and β-catenin from desmosomes. J Biol Chem. 2009; 284:31776–31788. [PubMed: 19759396]

Clarke EJ, Allan VJ. Cytokeratin intermediate filament organisation and dynamics in the vegetal cortex of living Xenopus laevis oocytes and eggs. Cell Motil Cytoskeleton. 2003; 56:13–26. [PubMed: 12905528]

Coulombe PA, Hutton ME, Vassar R, Fuchs E. A function for keratins and a common thread among different types of epidermolysis bullosa simplex diseases. J Cell Biol. 1991; 115:1661–1674. [PubMed: 1721910]

Davidson LA, Hoffstrom BG, Keller R, DeSimone DW. Mesendoderm extension and mantle closure in Xenopus laevis gastrulation: combined roles for integrin α5β1, fibronectin, and tissue geometry. Dev Biol. 2002; 242:109–129. [PubMed: 11820810]

Davidson LA, Keller R, DeSimone D. Patterning and tissue movements in a novel explant preparation of the marginal zone of Xenopus laevis. Gene Expr Patterns. 2004; 4:457–466. [PubMed: 15183313]

Desai RA, Gao L, Raghavan S, Liu WF, Chen CS. Cell polarity triggered by cell-cell adhesion via E-cadherin. J Cell Sci. 2009; 122:905–911. [PubMed: 19258396]

Dupin I, Camand E, Etienne-Manneville S. Classical cadherins control nucleus and centrosome position and cell polarity. J Cell Biol. 2009; 185:779–786. [PubMed: 19487453]

Farooqui R, Fenteany G. Multiple rows of cells behind an epithelial wound edge extend cryptic lamellipodia to collectively drive cell-sheet movement. J Cell Sci. 2005; 118:51–63. [PubMed: 15585576]

Franz JK, Franke WW. Cloning of cDNA and amino acid sequence of a cytokeratin expressed in oocytes of Xenopus laevis. Proc Natl Acad Sci U S A. 1986; 83:6475–6479. [PubMed: 2428034]

Franz JK, Gall L, Williams MA, Picheral B, Franke WW. Intermediate-size filaments in a germ cell: Expression of cytokeratins in oocytes and eggs of the frog Xenopus. Proc Natl Acad Sci U S A. 1983; 80:6254–6258. [PubMed: 6194528]

Haas P, Gilmour D. Chemokine signaling mediates self-organizing tissue migration in the zebrafish lateral line. Dev Cell. 2006; 10:673–680. [PubMed: 16678780]

Hammer Ø, Harper DAT, Ryan PD. PAST: Paleontological Statistics Software Package for Education and Data Analysis. Palaeontologia Electronica. 2001; 4:9.

Heasman J, Ginsberg D, Geiger B, Goldstone K, Pratt T, Yoshida-Noro C, Wylie C. A functional test for maternally inherited cadherin in Xenopus shows its importance in cell adhesion at the blastula stage. Development. 1994; 120:49–57. [PubMed: 8119131]

Helfand BT, Mendez MG, Murthy SN, Shumaker DK, Grin B, Mahammad S, Aebi U, Wedig T, Wu YI, Hahn KM, et al. Vimentin organization modulates the formation of lamellipodia. Mol Biol Cell. 2011; 22:1274–1289. [PubMed: 21346197]

Hirano S, Nose A, Hatta K, Kawakami A, Takeichi M. Calcium-dependent cell-cell adhesion molecules (cadherins): subclass specificities and possible involvement of actin bundles. J Cell Biol. 1987; 105:2501–2510. [PubMed: 3320048]

Hofmann I, Franke WW. Heterotypic interactions and filament assembly of type I and type II cytokeratins in vitro: viscometry and determinations of relative affinities. Eur J Cell Biol. 1997; 72:122–132. [PubMed: 9157008]

Keller RE, Schoenwolf GC. An SEM study of cellular morphology, contact, and arrangement, as related to gastrulation in Xenopus laevis. Wilhelm Roux's Archives Dev Biol. 1977; 182:165–186.

Kitt KN, Nelson WJ. Rapid suppression of activated Rac1 by cadherins and nectins during de novo cell-cell adhesion. PLoS One. 2011; 6:e17841. [PubMed: 21412440]

Klymkowsky MW, Shook DR, Maynell LA. Evidence that the deep keratin filament systems of the Xenopus embryo act to ensure normal gastrulation. Proc Natl Acad Sci U S A. 1992; 89:8736–8740. [PubMed: 1382297]

Kolega J. The movement of cell clusters in vitro: morphology and directionality. J Cell Sci. 1981; 49:15–32. [PubMed: 7031070]

Kowalczyk AP, Bornslaeger EA, Borgwardt JE, Palka HL, Dhaliwal AS, Corcoran CM, Denning MF, Green KJ. The amino-terminal domain of desmoplakin binds to plakoglobin and clusters desmosomal cadherin-plakoglobin complexes. J Cell Biol. 1997; 139:773–784. [PubMed: 9348293]

Kowalczyk AP, Navarro P, Dejana E, Bornslaeger EA, Green KJ, Kopp DS, Borgwardt JE. VE-cadherin and desmoplakin are assembled into dermal microvascular endothelial intercellular junctions: a pivotal role for plakoglobin in the recruitment of desmoplakin to intercellular junctions. J Cell Sci. 1998; 111(Pt 20):3045–3057. [PubMed: 9739078]

Kreplak L, Herrmann H, Aebi U. Tensile properties of single desmin intermediate filaments. Biophys J. 2008; 94:2790–2799. [PubMed: 18178641]

Ladoux B, Anon E, Lambert M, Rabodzey A, Hersen P, Buguin A, Silberzan P, Mege RM. Strength dependence of cadherin-mediated adhesions. Biophys J. 2010; 98:534–542. [PubMed: 20159149]

le Duc Q, Shi Q, Blonk I, Sonnenberg A, Wang N, Leckband D, de Rooij J. Vinculin potentiates E-cadherin mechanosensing and is recruited to actin-anchored sites within adherens junctions in a myosin II-dependent manner. J Cell Biol. 2010; 189:1107–1115. [PubMed: 20584916]

Leonard M, Chan Y, Menko AS. Identification of a novel intermediate filament-linked N-cadherin/γ-catenin complex involved in the establishment of the cytoarchitecture of differentiated lens fiber cells. Dev Biol. 2008; 319:298–308. [PubMed: 18514185]

Liu Z, Tan JL, Cohen DM, Yang MT, Sniadecki NJ, Ruiz SA, Nelson CM, Chen CS. Mechanical tugging force regulates the size of cell-cell junctions. Proc Natl Acad Sci U S A. 2010; 107:9944–9949. [PubMed: 20463286]

Long HA, Boczonadi V, McInroy L, Goldberg M, Maatta A. Periplakin-dependent re-organisation of keratin cytoskeleton and loss of collective migration in keratin-8-downregulated epithelial sheets. J Cell Sci. 2006; 119:5147–5159. [PubMed: 17158917]

Mammoto T, Ingber DE. Mechanical control of tissue and organ development. Development. 2010; 137:1407–1420. [PubMed: 20388652]

Maniotis AJ, Chen CS, Ingber DE. Demonstration of mechanical connections between integrins, cytoskeletal filaments, and nucleoplasm that stabilize nuclear structure. Proc Natl Acad Sci U S A. 1997; 94:849–854. [PubMed: 9023345]

Maruthamuthu V, Sabass B, Schwarz US, Gardel ML. Cell-ECM traction force modulates endogenous tension at cell-cell contacts. Proc Natl Acad Sci U S A. 2011; 108:4708–4713. [PubMed: 21383129]

McDonald JA, Pinheiro EM, Montell DJ. PVF1, a PDGF/VEGF homolog, is sufficient to guide border cells and interacts genetically with Taiman. Development. 2003; 130:3469–3478. [PubMed: 12810594]

Moore SW, Roca-Cusachs P, Sheetz MP. Stretchy proteins on stretchy substrates: the important elements of integrin-mediated rigidity sensing. Dev Cell. 2010; 19:194–206. [PubMed: 20708583]

Nagel M, Tahinci E, Symes K, Winklbauer R. Guidance of mesoderm cell migration in the Xenopus gastrula requires PDGF signaling. Development. 2004; 131:2727–2736. [PubMed: 15128658]

Nakatsuji N. Studies on the gastrulation of amphibian embryos: Cell movement during gastrulation in Xenopus laevis embryos. Wilhelm Roux's Archives Dev Biol. 1975; 178:1–14.

Nakatsuji N, Johnson KE. Cell locomotion in vitro by Xenopus laevis gastrula mesodermal cells. Cell Motil. 1982; 2:149–161. [PubMed: 7172219]

Nieuwkoop, PD.; Faber, J. Normal Table of Xenopus laevis (Daudin). New York: Garland Publishing Inc; 1994.

Prasad M, Montell DJ. Cellular and molecular mechanisms of border cell migration analyzed using time-lapse live-cell imaging. Dev Cell. 2007; 12:997–1005. [PubMed: 17543870]

Schwartz MA, DeSimone DW. Cell adhesion receptors in mechanotransduction. Curr Opin Cell Biol. 2008; 20:551–556. [PubMed: 18583124]

Theisen CS, Wahl JK 3rd, Johnson KR, Wheelock MJ. NHERF links the N-cadherin/catenin complex to the platelet-derived growth factor receptor to modulate the actin cytoskeleton and regulate cell motility. Mol Biol Cell. 2007; 18:1220–1232. [PubMed: 17229887]

Theveneau E, Marchant L, Kuriyama S, Gull M, Moepps B, Parsons M, Mayor R. Collective chemotaxis requires contact-dependent cell polarity. Dev Cell. 2010; 19:39–53. [PubMed: 20643349]

Todorovic V, Desai BV, Schroeder Patterson MJ, Amargo EV, Dubash AD, Yin T, Jones JC, Green KJ. Plakoglobin regulates cell motility through Rho- and fibronectin-dependent Src signaling. J Cell Sci. 2010

Torpey N, Wylie CC, Heasman J. Function of maternal cytokeratin in Xenopus development. Nature. 1992; 357:413–415. [PubMed: 1375708]

Trepat X, Wasserman MR, Angelini TE, Millet E, Weitz DA, Butler JP, Fredberg JJ. Physical forces during collective cell migration. Nat Phys. 2009; 5:426–430.

Winklbauer R. Mesodermal cell migration during Xenopus gastrulation. Dev Biol. 1990; 142:155–168. [PubMed: 2227092]

Winklbauer R, Selchow A, Nagel M, Angres B. Cell interaction and its role in mesoderm cell migration during Xenopus gastrulation. Dev Dyn. 1992; 195:290–302. [PubMed: 1304824]

Wolf K, Wu YI, Liu Y, Geiger J, Tam E, Overall C, Stack MS, Friedl P. Multi-step pericellular proteolysis controls the transition from individual to collective cancer cell invasion. Nat Cell Biol. 2007; 9:893–904. [PubMed: 17618273]

Wong P, Coulombe PA. Loss of keratin 6 (K6) proteins reveals a function for intermediate filaments during wound repair. J Cell Biol. 2003; 163:327–337. [PubMed: 14568992]

Yamada S, Wirtz D, Coulombe PA. Pairwise assembly determines the intrinsic potential for self-organization and mechanical properties of keratin filaments. Mol Biol Cell. 2002; 13:382–391. [PubMed: 11809846]

Yang X, Chrisman H, Weijer CJ. PDGF signalling controls the migration of mesoderm cells during chick gastrulation by regulating N-cadherin expression. Development. 2008; 135:3521–3530. [PubMed: 18832396]

Yonemura S, Wada Y, Watanabe T, Nagafuchi A, Shibata M. α-Catenin as a tension transducer that induces adherens junction development. Nat Cell Biol. 2010; 12:533–542. [PubMed: 20453849]

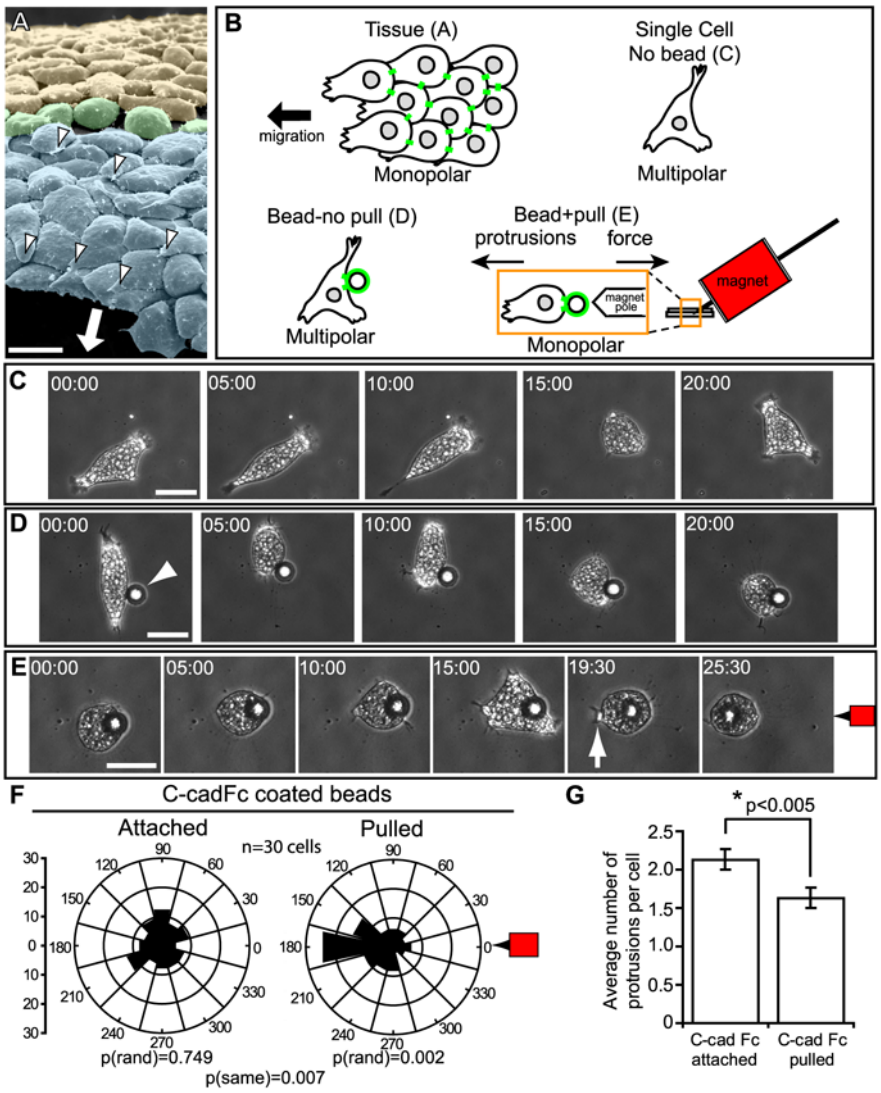

Figure 1. Force Application to Cadherin Induces Oriented Monopolar Protrusive Behavior

(A) SEM of mesendoderm (blue shading) from dorsal region of *Xenopus* gastrula with overlying blastocoel roof and attached FN matrix removed reveals basal surfaces of the mesendoderm cells with underlapping monopolar lamelliform protrusions (white arrowheads) oriented in the direction of travel (arrow). A transitional group of non-polar cells (green shading) separates mesendoderm and mediolaterally intercalating mesoderm (yellow shading). Note that the long axis of each mesendoderm cell (i.e., in direction of travel) is oriented perpendicular to that of the mediolaterally intercalating mesoderm cells. (B) Schematic of experimental strategy for magnetic bead pull assay (see Experimental Procedures for details). (C) Still images from timelapse movie (Movie S1) of a single multipolar mesendoderm cell plated on FN. (D) Still images from timelapse movie (Movie S2) of an isolated mesendoderm cell, plated on FN and with C-cadFc coated bead attached (arrowhead). (E) Still images from timelapse movie (Movie S2). Same cell as (D), C-cadFc bead pulled by magnet indicated at right (red magnet icon). A lamellipodium forms (arrow) opposite the direction of bead pull and results in directed cell migration. (F) Quantitation of protrusion angles relative to cell centroid (center of rose diagram) and magnet at right (0°). Y-axis for rose diagram represents percent of total protrusions. (G) Quantitation of

protrusions per cell after bead attachment and pull. Data are represented as mean ± SEM. All scale bars, 50μm. (C-E) Times shown in minutes:seconds. See also Figures S1, S2, and Movies S1-S3.

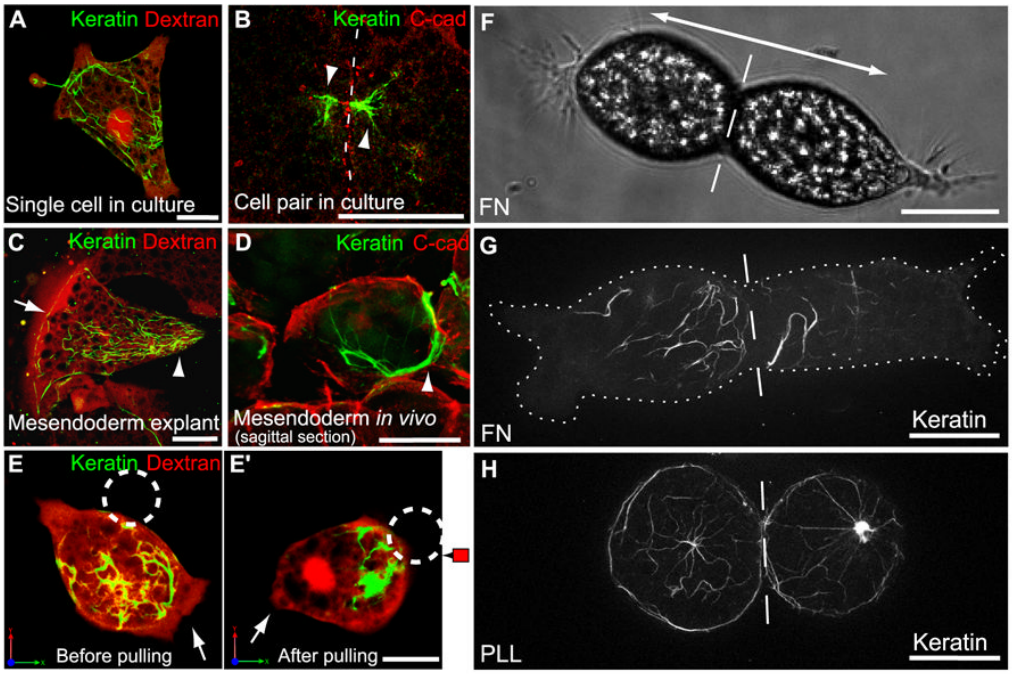

Figure 2. Keratin Organization is Regulated by Tension on Cell-Cell Contacts

(A) Single cell on FN, labeled with Alexa555-dextran (red) and expressing GFP-XCK1(8) to visualize KIFs (green). (B) Pair of fixed mesendoderm cells immunostained for C-cadherin (red) and XCK1(8) (green). Dashed line, cell-cell boundary. (C) Cell within mesendoderm tissue explant on FN labeled with Alexa555-dextran (red) and expressing GFP-XCK1(8) (green). (D) Sagittal perspective of mesendoderm cell in bisected embryo immunostained for C-cadherin (red) and XCK1(8) (green). KIFs in posterior of polarized cells (arrowheads B-D) and along tissue leading edge (arrow in C). (E,E') Single mesendoderm cell on FN labeled with Alexa555-dextran (red), expressing GFP-XCK1(8) (green). C-cadFc bead (dashed circle) attached to cell (E), then pulled for 20 min (E'). Arrows, leading edge protrusion. (F) Brightfield image of cell pair on FN, polarized in opposing directions (double arrow). (G,H) Cell pairs expressing GFP-XCK1(8), plated on FN (G) or PLL (H). Dashed line, cell-cell boundary. Cell borders outlined by dotted line in (G). All scale bars, 25μm. See also Movie S4.

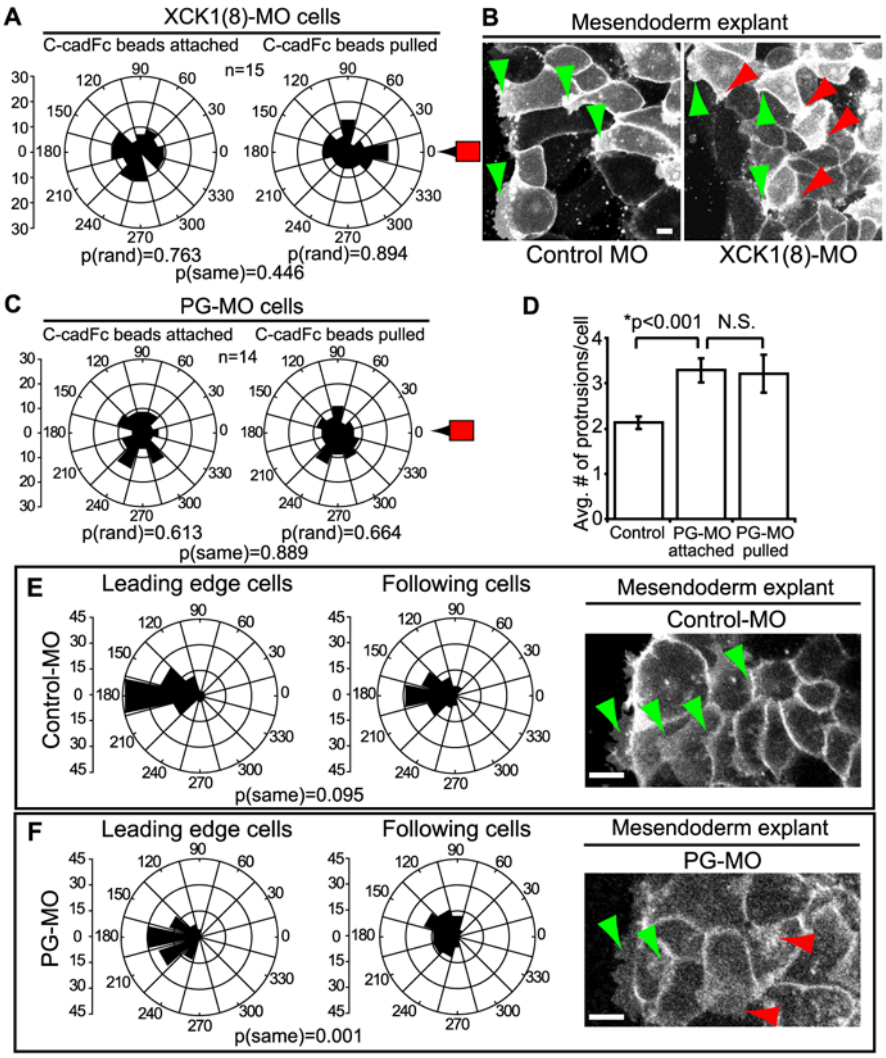

Figure 3. Keratin and PG are Required for Polarized Protrusive Behaviors

(A) Quantitation of protrusion angles from XCK1(8) morphant cells with C-cadFc beads attached and following bead pull. See also Figure S3 and Movie S5. (B) GAP43-GFP labels plasma membranes in intact mesendoderm explants prepared from control morphant (left) and XCK1(8) morphant embryos (right). Green arrowheads indicate protrusions in the direction of tissue movement and red arrowheads mark protrusions in any other direction. See also Movie S6. (C) Quantitation of protrusion angles from PG morpholino knockdown cells with C-cadFc beads attached and following bead pull. See also Figure S4 and Movie S7. (D) Quantitation of protrusion number per cell in normal and PG morphant cells. Data are represented as mean ± SEM. (E,F) Quantitation of protrusion angles, where 180° equals direction of tissue migration, in control morphant explants (E) and PG morphant explants (F). Leading cells = row 1, following cells = rows 2-4. In panels at right, GAP43-GFP labels plasma membrane of mesendoderm explants from control morphant and PG morphant embryos. See also Movie S8. Green arrowheads indicate protrusions in the expected direction of tissue movement and red arrowheads mark protrusions in any other direction. All scale bars, 25μm.

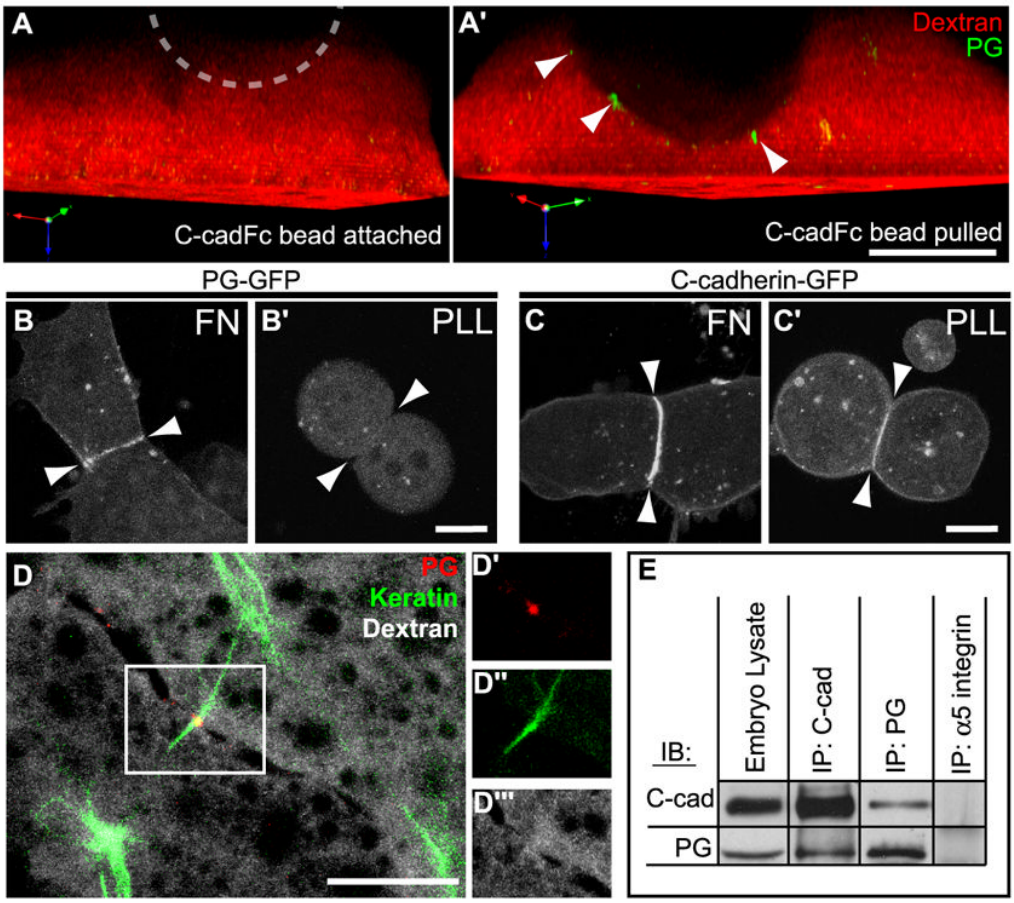

Figure 4. Recruitment of PG to Stressed Cadherin Adhesions

(A, A') 3D rendered side view of a normal cell injected with Alexa555-dextran (red) and expressing PG-GFP (green) before (A) and after (A') C-cadFc bead pull. Location of bead, dashed circle. Cells expressing either PG-GFP (B,B') or C-cadherin-GFP (C,C'), plated on either FN (B,C) or PLL (B',C') and allowed to form cohesive pairs. Arrowheads indicate plane of cell-cell boundaries. (D) Mesendoderm cells in live tissue expressing PG-GFP (red), mCherry-XCK1(8) (green), and labeled with Alexa647-dextran (gray). Image is a collapsed 2μm Z-stack of the posterior-lateral region of two adjacent cells in a mesendoderm explant. Outlined region in (D) is shown in independent color channels of plakoglobin-GFP (D'), mCherry-XCK1(8) (D"), and dextran (D'"). (E) C-cadherin and PG were immunoprecipitated from whole embryo extracts and immunoblotted as indicated. α5 integrin immunoprecipitates served as negative controls. All scale bars, 15μm.

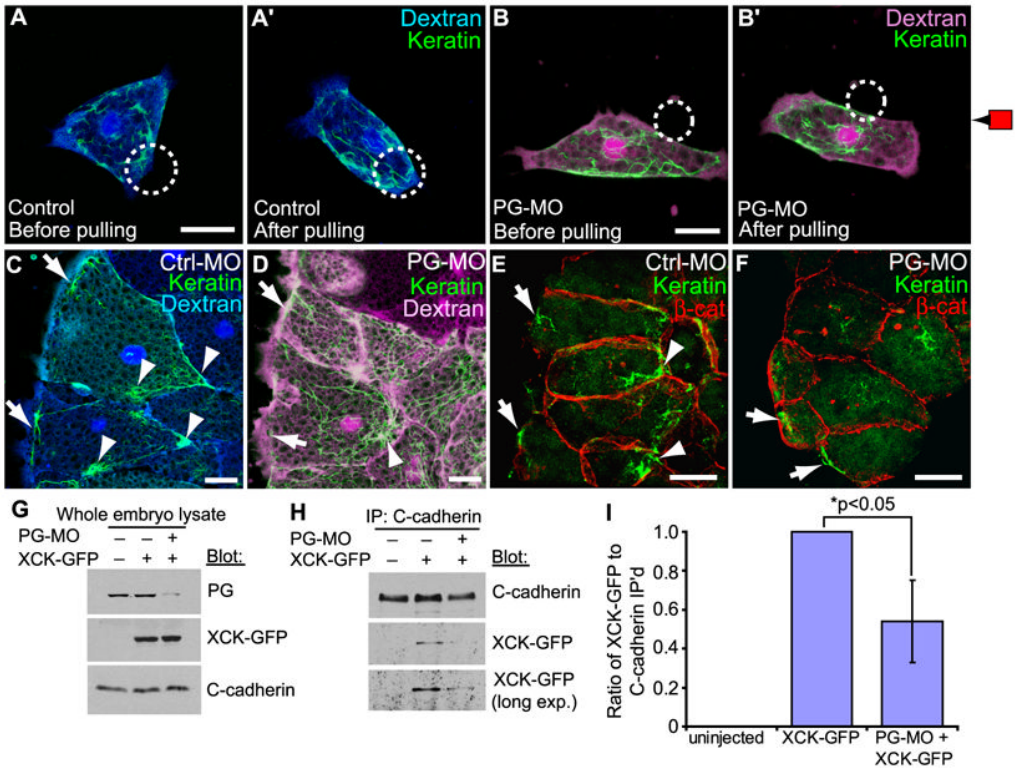

Figure 5. Requirement of PG for Cadherin/Keratin Association

(A,B) Single cells labeled with Alexa-dextran, expressing GFP-XCK1(8) (green) and plated on FN. (A,A') is a normal cell (blue dextran) and (B,B') is a PG morphant cell (magenta dextran). C-cadFc bead (circle) bound (A,B), then pulled (A',B'). (C) Control morphant (blue dextran) and (D) PG morphant (magenta dextran) mesendoderm tissue explants expressing GFP-XCK1(8) (green). See also Movie S8 and Figure S5. (E) Control and (F) PG morphant mesendoderm in whole embryos immunostained for XCK1(8) (green) and β-catenin (red). (C-F) Arrows, cabling along anterior of leading edge cells. Arrowheads, KIF aggregation near cell-cell contacts. All scale bars, 25μm. (G-I) Embryos were injected with XCK1(8)-GFP, with or without PG morpholino. (G) Immunoblots of embryo lysates show expression levels of XCK1(8)-GFP and endogenous PG with or without PG morpholino (PG-MO). (H) C-cadherin immunoprecipitates immunoblotted for XCK1(8)-GFP and C-cadherin with or without PG-MO. (I) Quantitation of three independent co-immunoprecipitation experiments shown as mean ± SEM.

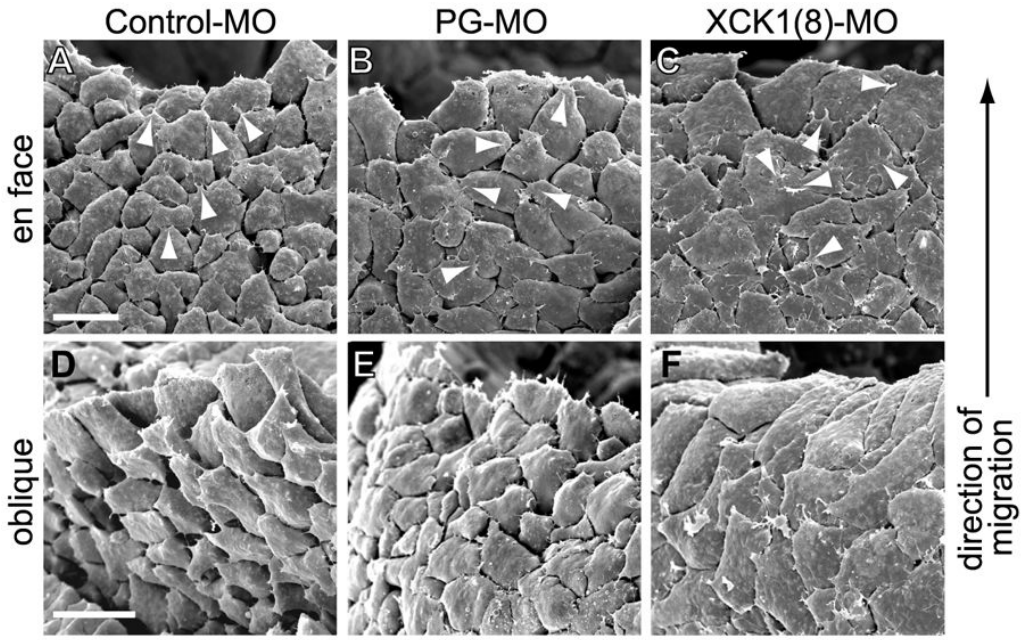

Figure 6. Requirement for PG and Keratin in Normal Mesendoderm *In Vivo*

Scanning electron micrographs of *Xenopus* embryos from which the overlying blastocoel roof was removed to reveal the basal aspect of the underlying mesendoderm (as in Figure 1A). Leading edge mesendoderm cells and direction of migration in all images is toward top. Images were acquired of (A,D) control morpholino injected embryos, (B,E) PG morpholino injected embryos, and (C,F) XCK1(8) morpholino injected embryos. En face view of basal aspect shown in (A-C) and oblique view of the basal surface shown in (D-F). Arrowheads indicate a sampling of cell protrusions. Scale bars, 50μm.

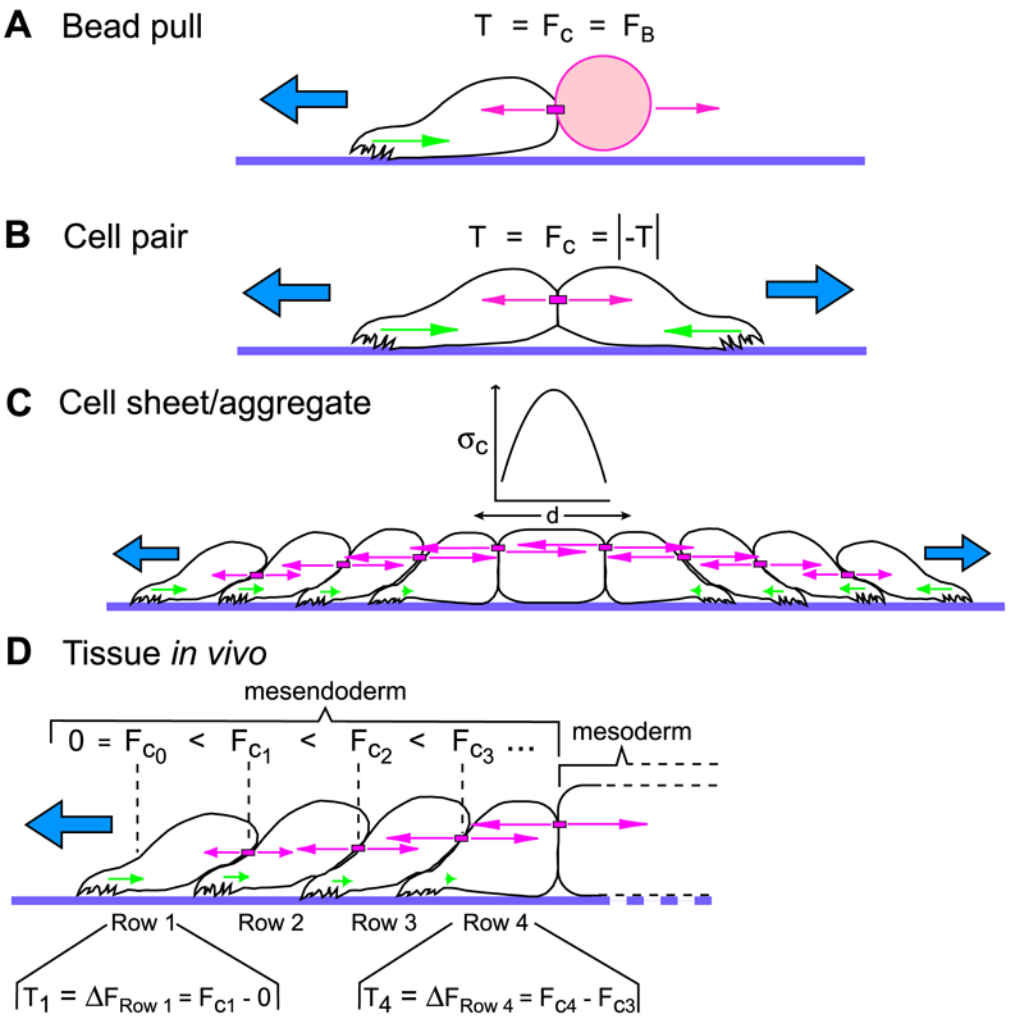

Figure 7. Model for Force-Induced Regulation of Cell Migration Polarity

(A) Applying tensile force on cadherins (F_C) in a single cell with a C-cadFc bead and magnetic tweezer mimics forces normally applied by neighboring cells in a multicelled array and induces a protrusion opposite the direction of applied force. When velocity is constant, net traction forces (T) exerted by the cell are necessarily equal to the force used to pull the bead (F_B). (B) Two cells that form a stable cell-cell contact polarize in opposite directions. Traction force that each cell exerts on the substrate (T) is balanced by an equivalent force at the cell-cell interface (F_C) to maintain cohesion. (C) In a cell sheet, stresses on cell-cell adhesions (σ_c, pink arrows) increase within the sheet and balance the traction stresses (green arrows) exerted by several rows of cells at the periphery of the sheet. Tractions at opposite margins of the cell sheet are opposed but equal, and the stress is borne between the tractive ends of the aggregate by intercellular adhesions (after Trepat et al., 2009). (D) Mesendoderm, like epithelial cell sheets *in vitro*, migrates via a distributed traction mechanism (Davidson et al., 2002). The traction forces that each cell exerts on the substrate must be balanced by the cell-cell adhesions that keep a cell part of a cohesive tissue. For the leader population of cells, this means that traction force (T_1) equals the force on the posterior cell-cell adhesion (F_{C1}). In follower cells that have cell-cell contacts at both the front and back, the difference between forces on the rearward cell-cell adhesion and forces on the forward cell-cell adhesion ($\Delta F_{Row\ x}$) is balanced by traction forces (T_x) (example

shown for row 4). In this model, the trailing mesoderm provides resistance to the cell-cell tension being generated by the advancing mesendoderm.